CURRENTS DRIVEN BY ELECTRON CYCLOTRON WAVES

C.F.F. KARNEY, N.J. FISCH
Plasma Physics Laboratory,
Princeton University,
Princeton, New Jersey,
United States of America

ABSTRACT. Certain aspects of the generation of steady-state currents by electron cyclotron waves are explored. A numerical solution of the Fokker-Planck equation is used to verify the theory of Fisch and Boozer and to extend their results into the non-linear regime. Relativistic effects on the current generated are discussed. Applications to steady-state tokamak reactors are considered.

1. INTRODUCTION

The generation of electric currents in a plasma by means of electron cyclotron wave absorption appears to be one of the more promising schemes of providing a steady-state toroidal current in a tokamak [1]. These waves can be employed to generate toroidal current merely by heating selected electrons and, interestingly, without directly injecting substantial toroidal momentum into these electrons. The wave launching structures are advantageously simple; since the wave need not have high parallel (to $\vec{B}$, the DC magnetic field) momentum content, its parallel phase velocity can be superluminous and, accordingly, no slow-wave structure is necessary. Moreover, the utilization of the high-frequency range (the wave frequency, ω, is comparable to Ω_e, the electron cyclotron frequency) implies that the wave power density is also high. It follows that free space waves of high power density may be injected into the plasma through conveniently small waveguide apertures in order to drive the toroidal current.

The main problem in generating current by this means is the power requirement, both in terms of the magnitude of the re-cycled power in a tokamak reactor and the capital costs of the equipment. Efficient CW power sources for this range of frequencies are yet to be developed. Assuming that these sources can be developed, the current must still be generated with minimal power dissipation for the scheme to be economically feasible in a fusion reactor. This minimization requires the absorption of the wave by only the fastest electrons, which are the most collisionless and hence retain their directed current longest. In this respect, this scheme is similar to the alternative technique of current generation by lower hybrid waves [2], which also exploits, among other things, the relative infrequency with which the superthermal electrons experience collisions. The present scheme, however, may allow the wave to resonate even with relativistic electrons [3] whereas the lower hybrid waves are constrained by an accessibility condition that, depending on the plasma β and temperature, allows resonance only with somewhat slower electrons.

It is an object of the present paper to analyse, both analytically and numerically, the mechanisms by which the absorption of electron cyclotron waves leads to the production of current. The paper is organized as follows: In Section 2, we consider analytically the wave absorption from the standpoint of linear theory in a slab-model low-density plasma. This simplified analysis nonetheless indicates the most promising injection angle of the wave into the tokamak and reasonably estimates the speed of the electrons that absorb the wave. In Section 3, we numerically check the formula given in Ref.[1] for J/P_d, the current generated per power dissipated, and we find close verification of the theory. We then turn to other effects that are likely to enter the problem in important parameter regimes. In Section 4, we consider non-linear effects, i.e. the effect that finite or even large wave power has on the amount of current generated and the wave damping rate. In Section 5, we assess the implications of relativistic effects [3] that become pertinent in reactor-grade plasmas. In Section 6, we present a summary of our findings.

Throughout our discussion we shall be comparing our observations with analytical and numerical treatments of the closely related and more familiar problem of current generation by lower hybrid waves [2, 4]
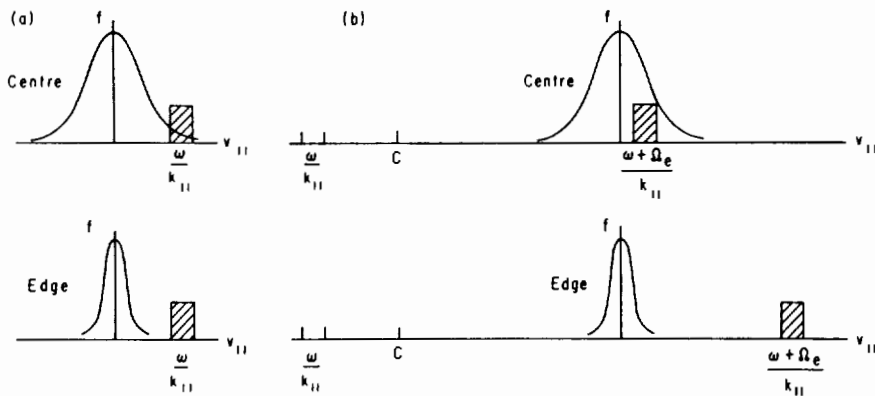
FIG.1. *Comparison of electron cyclotron and lower-hybrid methods of current drive. The wave spectrum and distribution function for the lower hybrid (a) and the electron cyclotron (b) methods of current drive.*

where the wave-particle interaction takes place at the Landau resonance. We conclude the present section with an important distinction between the two mechanisms. The resonance condition for electrons to exchange energy with the waves is

$$\omega - k_\parallel v_\parallel = n\Omega_e (s)$$

where $k_\parallel$ is the wave parallel wavenumber, $v_\parallel$ is the electron parallel velocity, s measures distance in the direction of the tokamak major radius and for lower hybrid waves n = 0, while for electron cyclotron waves n = ±1. It may be seen that, neglecting the poloidal magnetic field and toroidal curvature effects, electrons with the same $v_\parallel$ absorb the lower hybrid wave. Near the plasma centre, the plasma is hotter and denser than near the plasma periphery, so the absorption can be concentrated there as there are more electrons there to absorb the wave. This situation is depicted in Fig.1a, where a spectrum of waves with purposefully high parallel phase velocity is utilized to avoid power absorption near the cool and underdense periphery.

In contrast, as electron cyclotron waves propagate into regions of different magnetic field, they not only resonate with more electrons, but they resonate with electrons of different parallel velocity. This is depicted in Fig.1b, which indicates the phenomenon in the case of the extraordinary wave, which is launched from the high-field side of the tokamak, where there are no resonant electrons. At some interior point, however, there may be a large number of resonant electrons. Just as for the lower-hybrid wave, as the wave propagates inward, more and more electrons become

resonant. In contrast, however, to the case of the lower-hybrid wave, the electrons becoming resonant are those that are slower and slower as the wave nears the resonant surface, $\omega = \Omega_e$. The slower electrons are less efficient to heat for generating currents so that it becomes critical that the electron cyclotron wave damps completely before $v_\parallel$ becomes too small.

2. WAVE ABSORPTION

The effect of electron cyclotron resonance heating is to increase primarily the perpendicular velocity of the resonant electrons. The velocity increase lies in this direction because the waves have very little parallel momentum content compared to energy content, so that when the wave is absorbed by an electron, the electron energy increases, but, by momentum conservation, its parallel momentum barely increases. That the waves themselves have little parallel momentum to impart to the electrons is a consequence of their superluminous parallel phase velocity. The energy in a wave is proportional to ω, while its momentum is proportional to $\vec{k}$. Since $\omega/k_\parallel > c$, the waves possess relatively little momentum.

Neglecting then the small parallel momentum of the wave (which vanishes in the limit $\omega/k_\parallel \to \infty$), we view the wave-particle interaction as a diffusive process in velocity space where

$$\frac{\partial f}{\partial t} = \frac{1}{v_\perp} \frac{\partial}{\partial v_\perp} v_\perp D_{rf} \frac{\partial}{\partial v_\perp} f \qquad (1)$$

where f is the electron velocity distribution and D_{rf} is the wave diffusion coefficient which may be written heuristically as $D_{rf} = \langle \Delta v_\perp^2 \rangle / \Delta t$, where Δv is the characteristic velocity change in an auto-correlation time Δt. The waves accelerate electrons through a perpendicular electric field, $E_\perp$. For extraordinary waves we may write

$$\Delta v_\perp \simeq \frac{e}{m} E_\perp \Delta t \qquad (2)$$

where e/m is the electron-charge-to-mass ratio. The correlation time of the waves is approximately given by

$$\Delta t \simeq \pi / \Delta k_\parallel v_\parallel \qquad (3)$$

where we have chosen the constant π so that

$$D_{rf} = \frac{\Delta v^2}{\Delta t} = \left(\frac{eE_\perp}{m}\right)^2 \frac{\pi}{v_\parallel \Delta k_\parallel} \qquad (4)$$

which is just the result derived in a more precise manner [5]. The power dissipated may be found from Eq.(1) as

$$P_d = \int \frac{1}{2} n_o m v_\perp^2 \frac{\partial f}{\partial t} d^3 \vec{v}$$

$$= 2 n_o m D_{rf} \int f \, d^3 \vec{v} \equiv 2 n_r m D_{rf} \qquad (5)$$

where we have integrated twice by parts to obtain the second equality, assuming that D_{rf} is independent of $v_\perp$ in a range in $v_\parallel$, and we define n_r as the number of resonant electrons. The interpretation of Eq.(5) is that the power dissipated depends directly on the number of resonant electrons. (This result is a consequence of taking D_{rf} to be independent of $v_\perp$.) In the linear limit, the distribution function is a Maxwellian and n_r and the damping rate are independent of D_{rf}. It is possible, however, that n_r could change because of non-linear effects. Should n_r increase, then the wave damping rate, with increasing D_{rf}, would increase rather then decrease, in contrast to the scaling in the case of lower-hybrid waves. It is difficult, however, to find n_r analytically. We do, however, explore numerically non-linear aspects of this problem in Section 4.

We consider now the implications of the linear theory on the efficiency of driving current. Using Eq.(4) and assuming $k_\parallel > k_\perp$, we may write the temporal damping of extraordinary waves as

$$\gamma = \frac{\pi \omega_{pe}^2}{k_\parallel \Delta v_\parallel} \frac{n_r}{n_o} \qquad (6)$$

where ω_{pe} is the electron plasma frequency, and n_r is the density of resonant electrons in a width $\Delta v_\parallel$. The spatial damping of the wave is given in the limit of underdense plasma as

$$\alpha_s = \frac{\gamma}{v_{gs}} = \frac{\gamma k}{c k_s} \simeq \frac{\pi}{k_s c} \frac{\omega_{pe}^2}{\Delta v_\parallel} \frac{n_r}{n_o} \qquad (7)$$

where the subscript s denotes the direction that is also parallel to ∇R, where R is the major radius.

It is important to determine the region of velocity space in which the largest portion of the wave energy is absorbed. The wave enters the plasma at some horizontal position $s = s_a$ and eventually loses its power at some position $s = s_b$. It may be imagined that at $s = s_a$ there are no or very few electrons resonant with the wave, whereas at $s = s_b$ there are a substantial number of electrons, hopefully with normalized parallel velocity $v_\parallel / v_{te} = w \gg 1$, that are resonant with the wave. Thus, s_b satisfies the equation

$$1 \simeq \int_{s_b}^{s_a} \alpha(s) \, ds \simeq \int_{s_b}^{\infty} \alpha(s) \, ds$$

$$\simeq \frac{\pi \omega_{pe}^2}{k_s c n_o \Delta v_\parallel} \int_{s_b}^{\infty} n_r \, ds \qquad (8)$$

The integral is perhaps more transparent in w-space where we write

$$\frac{n_r}{n_o} = \frac{\Delta w}{\sqrt{2\pi}} e^{-w^2/2} \qquad (9)$$

and

$$\frac{dw}{ds} = \frac{1}{v_{te}} \frac{d}{ds} \left[\frac{\omega - \Omega_e(s)}{k_\parallel} \right] = \frac{\Omega_e}{k_\parallel R v_{te}} \qquad (10)$$

so that Eq.(8) becomes

$$1 \simeq \sqrt{\frac{\pi}{2}} \left(\frac{k_\parallel}{k_s}\right)\left(\frac{\omega_{pe}}{\Omega_e}\right)\left(\frac{R}{c/\omega_{pe}}\right) \frac{e^{-w^2/2}}{w} \qquad (11)$$

where w is the normalized resonant parallel velocity at $s = s_b$.

of the esonant ave nears ctrons are so that it wave all.

heating ocity of lies in tle rgy y an by tum have little is is a phase al to ω, nce omentum. um of the we view rocess in

(1)

For a fusion-grade plasma, it is easily seen from Eq.(11) that $w \gtrsim 4$ is attainable, consistently with full damping of the extraordinary wave. Further optimization (i.e. damping at higher w) can be obtained by minimizing k_s for a given $k_{\parallel}$. This corresponds to angling the wave not only in the toroidal direction, but also in the vertical direction as it enters the plasma.

Let us note that because of the exponential dependence on w, nearly all the wave energy is absorbed in a narrow range Δw in w. This corresponds to a narrow width Δs in s. To estimate the damping width Δs, consider that a Maxwellian exponentiates in a width $\Delta w = 1/w$. Thus, making use of Eq.(10), we find that $\Delta s = k_{\parallel} R v_{te} \Delta w / \Omega_e$, or, in normalized parameters,

$$\frac{\Delta s}{a} \simeq \frac{0.1}{T_{10}^{1/2}} \left(\frac{R}{3a}\right)$$

where a is the minor radius and T_{10} is the temperature normalized to 10 keV. In the regime $T_{10} \gtrsim 1$, pertinent to reactors, it is seen that $\Delta s/a$ is indeed small. The heating and current generation profiles can, however, be much broader than is apparent at first glance. This is because Δs only measures distance parallel to ∇R. In fact, by vertically angling the wave ($k_s \ll k_{\perp}$), not only is the current generated at higher w, but the deposition profile is broader since the wave damping now occurs over a longer length that intersects many magnetic surfaces.

To determine which is actually the best configuration for current generation, a full propagation study, such as has been conducted for the heating profile [6], would have to be undertaken. Note that for a given plasma (i.e. density and temperature profiles and dimensions) there is the opportunity to vary five wave parameters: the frequency, which determines the vertical resonance surface; the poloidal angle at which the waveguide intersects the plasma periphery; the angles of injection, both in the toroidal direction and in the vertical direction; and, finally, the fifth parameter is the narrowness of the wave spectrum for a given power. The power is given roughly by the amount of current to be generated. The fifth parameter involved in the optimization dictates whether this power is to be concentrated in a narrow spectrum of $k_{\parallel}$ or not.

3. CHECK OF THE LINEAR THEORY

A formula was derived in Ref. [1] for the quantity J/P_d for the case where the waves push electrons at velocities much exceeding the thermal velocity. This analysis represented a significant advance on the previous one-dimensional theory [2] in that it distinguishes the scattering of electrons in pitch angle and energy. Furthermore, it treats the case of electron cyclotron damping which was not covered by the one-dimensional treatment. The important approximation made in Ref.[1] was the neglect of diffusion in the energy direction. (Slowing-down only was included in this direction.) The derivation itself is only valid when the speed of the resonant electrons far exceeds the electron thermal speed. We now seek to check the theoretical result of Ref. [1] by computing J/P_d from a numerical solution of the two-dimensional Fokker-Planck equation.

The Fokker-Planck program used is the same as described in Refs [4, 7]. That is, it solves

$$\frac{\partial}{\partial \tau} f = \frac{\partial}{\partial \vec{u}} \overset{\leftrightarrow}{D}_{rf} \frac{\partial}{\partial \vec{u}} f + \frac{\partial f}{\partial \tau}\bigg|_{coll} \tag{12}$$

where $\overset{\leftrightarrow}{D}_{rf}$ is the wave diffusion tensor (a function of $\vec{v}$) and the collision term $\partial f/\partial t|_{coll}$ is calculated assuming fixed, constant-temperature backgrounds of electrons and ions. As before, we adopt a normalization where

$$\tau = \nu_o t \qquad [\nu_o = \log \Lambda \, \omega_{pe}^4/(2\pi n_o v_{te}^3)]$$

$$\vec{u} = \vec{v}/\vec{v}_{te} \quad (v_{te}^2 = T_e/m)$$

Normalized current and power dissipation are measured in units of $en_0 v_{te}$ and $\nu_0 n_0 T_e$, respectively. In addition, we define x and w to be the perpendicular and parallel (to $\vec{B}_0$) components of $\vec{u}$. The domain of integration is $u \leqslant 10$, with the condition that there be no flux of particles normal to the boundary. Normally, we shall only be concerned with cases where only the $\vec{x}\vec{x}$ (cyclotron damping) or the $\vec{w}\vec{w}$ (Landau damping) component of $\overset{\leftrightarrow}{D}$ is non-zero.

With these normalizations J/P_d is predicted to be [1]

$$\frac{J}{P_d} = \frac{\hat{S} \cdot \nabla(wu^3)}{\hat{S} \cdot \nabla u^2} \frac{4}{5 + z_i} \tag{13}$$

where $\vec{S}$ is a unit vector in the direction in which the wave pushes the electrons (i.e. $\vec{S} = \vec{x}$ for cyclotron damping and $\vec{S} = \vec{w}$ for Landau damping) and Z_i is the ion charge state. In practice, Eq.(13) should be integrated over the spectrum of waves. A further complication arises if the waves are strong enough to
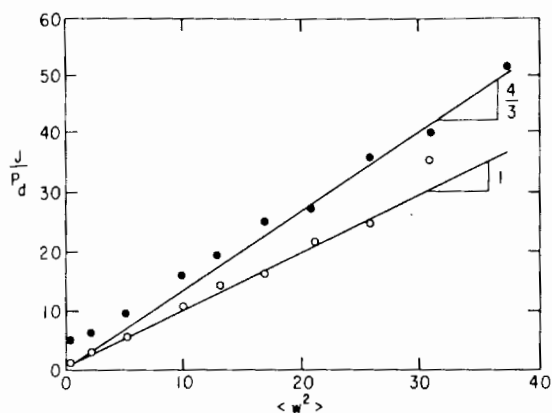
FIG.2. J/P_d for small D as a function of $\langle w^2 \rangle$ where $D = 10^{-3}$, $w_2 - w_1 = 1$. The waves exist only for $x < 1$. Open circles denote cyclotron damping and closed circles Landau damping. Lines show the theoretical predictions of Eq.(13).

. This
ie pre-
inguishes
iergy.
otron
nensional
e in
gy
i this
hen the
electron
retical
merical
equation.
: as

(12)

ion of
l
inds of
nalization

)]

measured
iddition,
parallel
gration
ux of
ve shall
$\vec{x}$
ing)

to be [1]

(13)

ch the
ion
Z_i is
ld be
ier
igh to

alter the distribution function f significantly because then f must be determined before Eq.(13) can be applied. These difficulties rule out a detailed comparison of Eq.(13) with the numerical results obtained for the Landau-damping case [4].

Here, we circumvent these difficulties by choosing $\vec{D}$ to be small and localized in velocity space. Although the localization of $\vec{D}$ may be difficult to realize, this approach does allow us to check the physics embodied in Eq.(13). We take $\vec{D}_{rf}$ to have a form which is zero except for $w_1 < w < w_2$ and $x < 1$, where it is equal to a constant D multiplying either $\vec{x}\vec{x}$ or $\vec{w}\vec{w}$. We take $w_2 - w_1 = 1$ and $D = 10^{-3}$. Figure 2 shows J/P_d plotted as a function of $\langle w^2 \rangle$, where the average is computed with a Maxwellian weighting, i.e.

$$\langle w^2 \rangle = \frac{\int_{w_1}^{w_2} w^2 \, f_M(w) dw}{\int_{w_1}^{w_2} f_M(w) dw}$$

where $f_M(w)$ is a Maxwellian distribution.

There is excellent agreement between the numerical results (the symbols) and the analytical predictions (the lines). Interestingly, the theory and numerical results appear to agree fairly well even with w small for the cyclotron damping case but not for the Landau damping case. This is because the parallel input of momentum begins to be very substantial for low-phase velocity waves [7] and J/P_d must begin to increase as $1/w$. This effect is not present for the ECRH. Note, however, that these numerical calcu-

lations were performed assuming the background electrons to be non-drifting. If this constraint is relaxed [7], the results for J/P_d for $w_{1,2} \lesssim 1$ should be increased by a factor of about two.

4. NON-LINEAR RESULTS

Normally, we shall be interested in cases where D_{rf} is large enough to perturb f significantly. To illustrate the type of behaviour we might expect, we show, in Fig.3, plots of f for $D \to \infty$ and $w_1 = 4$, $w_2 = 5$, for the cases of cyclotron and Landau damping. (As in the previous section, we take D_{rf} to be a constant D for $w_1 < w < w_2$. The perpendicular extent of the waves was determined only by the integration region, $u \leqslant 10$.)

A novel method was developed to treat the case of $D \to \infty$. This is based on the observation that $\vec{S} \cdot \partial f / \partial \vec{v}$ must be zero. (Recall $\vec{S}$ is the direction in which the waves accelerate the particles.) This is achieved by replacing the diffusion operator by an averaging operator where the averaging is performed in strips aligned with $\vec{S}$.

Returning to Fig.3, we first of all note that the perturbation to f is much greater in the cyclotron damping case. The reason for this is that the waves accelerate the particles so that they tend to stay in the
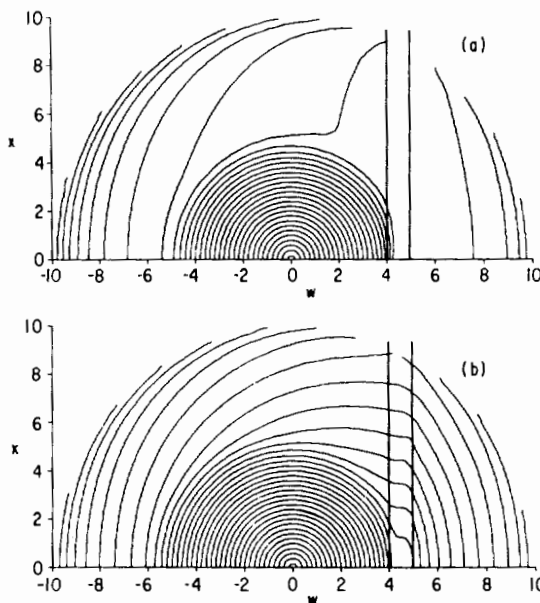

FIG.3. Steady-state distribution functions for $D \to \infty$ with $w_1 = 4$, and $w_2 = 5$. Figures (a) and (b) show the cases of electron cyclotron waves and lower-hybrid waves, respectively.

resonant region. The waves are, therefore, more effective at accelerating the particles than waves which interact with particles via the Landau resonance. The greater perturbation in the cyclotron damping case means first that more current is generated (for Fig.3, $J = 3 \times 10^{-3}$ for cyclotron damping and 6×10^{-4} for Landau damping). Since much of this current is carried by relatively collisionless particles with high perpendicular velocity, J/P_d is approximately twice its value in the low-D limit. (For $w_1 = 4$ and $w_2 = 5$, $J/P_d = 37$ for $D \to \infty$, while $J/P_d = 17$ for $D \to 0$.) In fact, the cyclotron-damped waves have caught up with the Landau-damped waves which at low D were more efficient in terms of J/P_d. (For Landau-damped waves with $w_1 = 4$ and $w_2 = 5$, $J/P_d = 37$ for $D \to \infty$ and $J/P_d = 26$ for $D \to 0$.)

The ease with which cyclotron-damped waves can perturb f has one interesting consequence, namely that the power dissipated by the wave does not necessarily saturate as D is increased. (P_d did saturate for the case shown in Fig.3 because of the effective cut-off on D at $u = 10$.) Such a saturation does occur with waves which are Landau-damped and results in the damping rate becoming zero as $D \to \infty$. With cyclotron-damped waves, the behaviour of the damping rate as D varies is a function of the $v_\perp$-dependence of D. In particular, even when D is large enough to greatly distort f, the damping rate may be fairly close to the linear damping rate.

Figure 4 shows J/P_d and P_d as functions of D for $w_1 = 4$ and $w_2 = 5$. As D is increased, J/P_d shows a steady rise while P_d is very nearly proportional to D, showing the constancy of the damping rate. This is so even though the distribution at the highest value of D given in Fig.4, $D = 0.25$, is far from a Maxwellian (see Fig.5). For comparison, the lower-hybrid case is illustrated in Fig.4 also. Note the strong saturation of P_d.

A corollary of the nearly linear behaviour of P_d with D is that the damping of a particular component of the wave spectrum is not greatly affected by the neighbouring components. This is illustrated in Table I where the cases of $(w_1, w_2) = (4, 5)$, $(5, 6)$, and $(4, 6)$ with $D = 0.1$ are compared. We see that J and P_d for the (4,6) case are given to within 10% by the sums of the (4, 5) and (5, 6) cases. On the other hand, the discrepancy with lower hybrid waves is a factor of about two.

The results presented in this section need to be taken with some caution because when D_{rf} is constant (as in these computations), there is a possibility of a runaway in the perpendicular direction since at high $v_\perp$ the collisions are not able to hold the electrons back
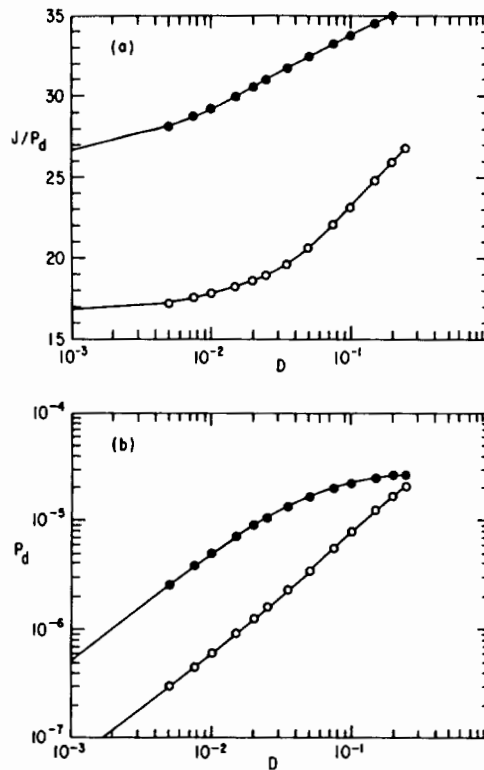

FIG.4. J/P_d (a) and P_d (b) as functions of D for $w_1 = 4$ and $w_2 = 5$. Open circles denote cyclotron damping and closed circles Landau damping.
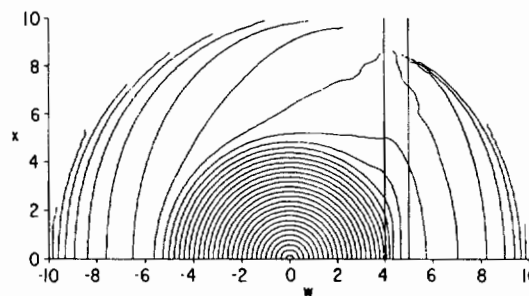

FIG.5. Steady-state distribution for $D = 0.25$, $w_1 = 4$, and $w_2 = 5$ (cyclotron damping).

effectively so that particles would be continuously accelerated in $v_\perp$, precluding the establishment of a steady state. The presence of the numerical cut-off of the waves at $u = 10$ would then dramatically alter the results. In practice, however, the finite perpendicular wavelength of the waves causes D to take a Bessel function dependence [5] so that $D_{rf} \sim 1/v_\perp$ for high $v_\perp$. (In the special case of linear polarization, there is a cancellation which results in $D_{rf} \sim 1/v_\perp^3$.)

TABLE I.
AND (4, 6
denote cy
column he
and (4, 6).

(w_1, w_2)
J_{cyc}
$P_{d,cyc}$
J_{th}
$P_{d,th}$

This decay
ensure the
assuming tl
diluted by
that the fra
occupied by
The effecti
same rate a:
Planck equ;
steady state

The $1/v_\perp$
For typical
would be x
$u = 10$, then
boundary w
since we kn
beyond the
on D_{rf}, we
To determir
values of D_r
important, '
the velocitie
light. This
section.

5.

In this sec
effects may
pertinent to
in the lower-
increasingly i
are character

TABLE I. J AND P_d FOR $(w_1, w_2) = (4, 5), (5, 6)$, AND $(4, 6)$, AND $D = 0.1$. The subscripts cyc and lh denote cyclotron waves and lower-hybrid waves. The column headed 'sum' is the sum of the columns $(4, 5)$ and $(4, 6)$.

(w_1, w_2)	$(4, 5)$	$(5, 6)$	sum	$(4, 6)$
J_{cyc}	1.7×10^{-4}	2.5×10^{-6}	1.8×10^{-4}	2.1×10^{-4}
$P_{d,cyc}$	7.9×10^{-6}	7.9×10^{-8}	8.0×10^{-6}	8.8×10^{-6}
J_{lh}	7.4×10^{-4}	1.1×10^{-5}	7.5×10^{-4}	1.4×10^{-3}
$P_{d,lh}$	2.2×10^{-5}	2.4×10^{-7}	2.2×10^{-5}	3.6×10^{-5}

This decay of D_{rf} is probably sufficiently fast to ensure the existence of a steady state. (We are assuming that at large $v_\perp$ the effectiveness of D_{rf} is diluted by the geometrical factor arising from the fact that the fraction of the velocity space shell at u occupied by the resonant region is proportional to $1/u$. The effective D_{rf} then decays as $1/u^2$ which is at the same rate as the frictional term in the Fokker-Planck equation. This allows the establishment of a steady state in which f decays exponentially with u.)

The $1/v_\perp$ dependence takes over at $v_\perp \sim \Omega_e/k_v \sim c$. For typical electron temperatures (~ 10 keV), this would be $x \sim 10$. If we solve for f with a boundary at $u = 10$, then the error entailed by introducing the boundary will be small if f at the boundary is small since we know that f, in fact, decays exponentially beyond the boundary. Since the decay rate depends on D_{rf}, we must also restrict D_{rf} from being too large. To determine the behaviour of the particles at larger values of D_{rf} where the large-$v_\perp$ behaviour of D_{rf} is important, we must include relativistic effects because the velocities of these particles are close to that of light. This problem will be discussed in the next section.

5. RELATIVISTIC EFFECTS

In this section, we outline how various relativistic effects may play a role. These effects, which are pertinent to fusion-grade plasmas, are all rather weak in the lower-temperature reactors ($T_{10} < 2$), but become increasingly important at the higher temperatures that are characteristic of more advanced reactors.

The most important relativistic effect relates to the efficiency of current generation. As is described in Ref. [3], this efficiency is somewhat reduced for mildly relativistic electrons, but approaches zero for very relativistic electrons. In view of this inefficiency of relativistic electrons, this effect supersedes the additive deleterious effect of power loss through synchrotron radiation of very fast electrons.

There are other relativistic effects that concern the wave-particle interaction itself. One effect is the decrease in D_{rf} due to finite-gyroradius effects, which is an effect available non-relativistically, too. We turn here, however, to more fundamentally relativistic effects. In our analysis, we assumed that electrons were pushed by the wave only in $v_\perp$-space where they remained in resonance with the wave. The result of this would be that, in the absence of collisional effects, there would be complete flattening in $v_\perp$ space for the resonant electrons, i.e. $f \to 0$. Relativistic effects change this picture in two ways. First of all, as the electron perpendicular energy increases, so does its relativistic mass, which means that it can fall out of resonance. To be specific, the resonance condition is now

$$v_\parallel = (\omega - \Omega_e/\gamma)/k_\parallel$$

where $\gamma = (1 - v^2/c^2)^{-1/2}$ and Ω_e is the cyclotron frequency of non-relativistic electrons. The result of the electron falling out of resonance is that the flattening in $v_\perp$ cannot continue and f will not vanish anywhere in the collisionless limit.

The second relativistic effect on the flattening of f relates to the direction in which electrons are diffused. This diffusion path may be thought of as that sector of velocity space where f is induced to be constant by the influence of a wave with parallel phase velocity $\omega/k_\parallel$. It is given by

$$E - p_\parallel \omega/k_\parallel = \text{const} \tag{14}$$

which is the relativistic statement of conservation of energy and parallel momentum. The effect of this is again to push electrons not purely in the perpendicular direction and hence to push them out of the resonance with the wave. Now, f becomes normalizable in the collisionless limit.

To appreciate Eq.(14), it is helpful to picture these diffusion paths. In the non-relativistic limit, Eq.(14) describes the familiar concentric circles in velocity space about the point $(v_\perp = 0, v_\parallel = \omega/k_\parallel)$. Consider, however, Fig.6a, where diffusion paths due to a wave at $\omega/k_\parallel = 0.6$ c are depicted. The familiar circles are
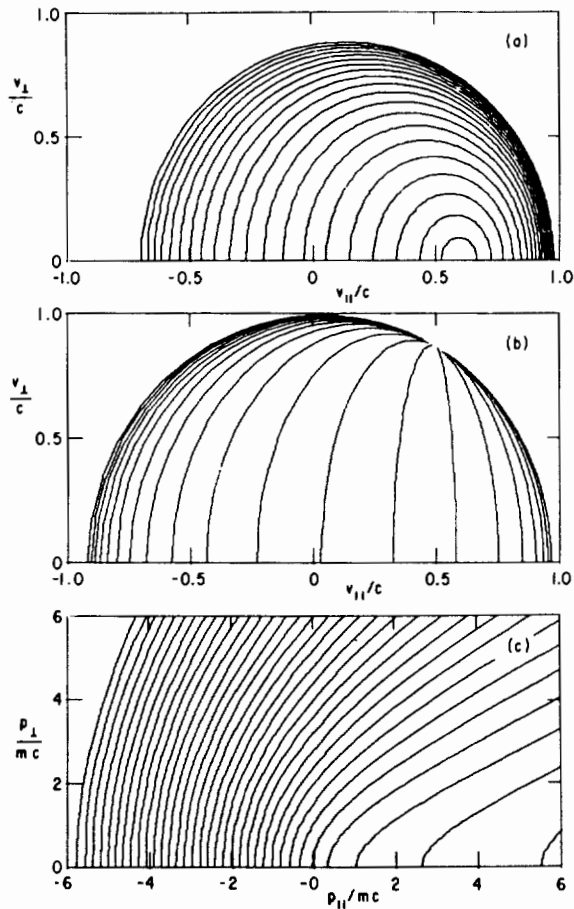
FIG.6. *Diffusion paths for particles in waves. Velocity space with (a) $\omega/k_{\parallel} = 0.6$ c, (b) $\omega/k_{\parallel} = 2$ c, (c) momentum space with $\omega/k_{\parallel} = 1.1$ c.*

now seen to be somewhat distorted in order to assure that the particle velocity remain less than c. In Fig.6b, we show diffusion paths due to a superluminous wave with $\omega/k_{\parallel} = 2$ c. Here, the topology of the paths is seen to have changed from ellipsoidal to hyperboloidal surfaces. The topology change is characteristic of superluminous waves and occurs in momentum space, too. In Fig.6c, we show the diffusion paths in momentum space for $\omega/k_{\parallel} = 1.1$ c.

We now turn to relativistic effects playing a role in technological considerations. From an engineering standpoint, it would be most preferable to use a wave of the lowest possible frequency and to inject it from the low-field side of the tokamak.

Let us first consider the launching of the extra-ordinary plasma wave which must be done from the high-field side of the tokamak. The resonance condition $k_{\parallel} v_{\parallel} = \omega - \Omega_e/\gamma$ may be written as

$$\left| \frac{\omega}{\Omega_e/\gamma} \right| = \left(1 + \frac{v_{\parallel}}{\omega/k_{\parallel}} \right)^{-1} \qquad (15)$$

and two implications with respect to minimizing ω become apparent. Note that $\omega/k_{\parallel} > c$; at reactor grade temperatures, however, $v_{\parallel}$ may approach c. Thus, we may bound

$$\frac{1}{2} < \frac{\omega}{\Omega_e/\gamma} < 1$$

and the lower (preferable) limit is accessible only for nearly parallel injection ($k_{\parallel} \gg k_{\perp}$) and absorption by relativistic electrons. This limit is preferred because it minimizes the frequency of the power source.

The second point to be made about Eq.(15) is that, for relativistic electrons, γ becomes large, which has the effect of requiring a lower-frequency power source.

For the ordinary wave, which is launched from the low-field side, similar considerations are pertinent. Here we have

$$\left| \frac{\omega}{\Omega_e/\gamma} \right| = \left(1 - \frac{k_{\parallel} v_{\parallel}}{\omega} \right)^{-1}$$

and, for this wave, small $k_{\parallel}$ implies smaller ω and $\omega > \Omega_e/\gamma$ is always true.

6. CONCLUSIONS

We have examined various aspects of current drive by electron cyclotron waves. Although the current drive mechanism is intrinsically less efficient than for current drive by lower hybrid waves, the greater flexibility of positioning the wave spectrum and the non-linear enhancement of J/P_d given in Section 4 offset this disadvantage.

The most interesting result of the numerical studies of the non-linear problem is that the damping rate of the wave is nearly independent of the power level. The weak dependence that exists is masked by the exponential factor $\exp(-w_1^2/2)$ entering the formula for the dissipated power. This means that ray-tracing codes may safely use linear damping theory. Non-linear effects become important in estimating the current drive efficiency, where the non-linearity can enhance J/P_d by up to a factor of about two.

For the current to be generated in a single direction, we require that all the power be absorbed before the cyclotron layer. In Section 2, it was shown that this was easily achieved with the extraordinary wave in a

reactor. An additional margin of safety is provided, however, by placing the source close to the top or bottom of the machine (but still in the high-field side of the cyclotron layer) since the group velocity normal to the cyclotron layer is, thereby, reduced. Such an arrangement also allows easier access for the waveguides.

We have presented here only the numerical results for the extraordinary wave for which D is independent of $v_\perp$ for low $v_\perp$. For the ordinary wave, the polarization of the wave is such that the electric field vector is rotating in the direction opposite to that of the electrons. The diffusion coefficient D then behaves as $v_\perp^4$ for low $v_\perp$. This is more difficult to model numerically because of the greater importance of an accurate treatment of the behaviour of large-$v_\perp$ particles. We expect that, for given w_1 and w_2, the efficiency of current generation will be greater because more of the current is carried by collisionless high-velocity particles. The damping rate is, however, also smaller so that more current will be generated at lower values of w_1.

Several phenomena affect the diffusion of electrons at high $v_\perp$. Finite-wavelength effects cause the diffusion coefficient to oscillate with a Bessel function dependence. Equally important, however, may be relativistic effects which change both the diffusion paths and the resonant region. Relativistic effects also allow the use of frequencies substantially below the cyclotron frequency. This will be important in hot second-generation reactors.

ACKNOWLEDGEMENTS

REFERENCES

[1] FISCH, N.J., BOOZER, A.H., Phys. Rev. Lett. 45 (1980) 720.
[2] FISCH, N.J., Phys. Rev. Lett. 41 (1978) 873; 42 (1979) 410.
[3] FISCH, N.J., Phys. Rev. A (to be published Dec. 1981).
[4] KARNEY, C.F.F., FISCH, N.J., Phys. Fluids 22 (1979) 1817.
[5] KENNEL, C.F., ENGELMANN, F., Phys. Fluids 9 (1966) 2377.
[6] OTT, E., HUI, B., CHU, K.R., Phys. Fluids 23 (1980) 1031.
[7] FISCH, N.J., KARNEY, C.F.F., Phys. Fluids 24 (1981) 27.